tance. Although we have demonstrated that Bcl-x_L forms an ion-selective channel, it is also possible that the relevant molecule that Bcl-x_L conducts in order to regulate apoptosis is not an ion. Cytochrome *c* is a protein that resides in the mitochondrial intermembrane space and its redistribution to the cytoplasm has been suggested to promote apoptosis through the activation of interleukin-1β-converting enzyme (ICE)-like proteases[20,21]. Although the pore-forming domain of diphtheria toxin forms an ion-conductive channel, one important function of this domain is to facilitate passage of another protein, the A fragment, through the endosomal membrane[6]. Thus, it is possible that Bcl-x_L also regulates the passage of proteins.

Using two independent methodologies, we have determined that Bcl-x_L forms an ion channel. This channel is pH-sensitive, cation-selective, and exhibits multiple conductance states with complex opening kinetics. These properties are similar to those reported for the pore-forming domain of one or more of the bacterial toxins that include diphtheria toxin, delta-endotoxin and colicins[6,7,22]. For example, similar to Bcl-x_L, diphtheria toxin becomes less cation selective at low pH, and low pH also enhances the channel activity of both diphtheria toxin and the colicins[6,7,23]. Like Bcl-x_L, delta-endotoxin and/or colicin E1 have been reported to have multiple conductance states with complex opening kinetics and comparable ion selectivities[7,22,24]. However, the collective channel properties of Bcl-x_L appear unique. Although Bcl-x_L shares structural and functional similarities with bacterial pore-forming domains, the ability of Bcl-x_L to promote cell survival may not result solely from its ability to form a channel. For example, although some eye lens crystallins have structural and functional similarities to metabolic or detoxification enzymes with which they are thought to share common ancestors, the shared enzymatic features are not sufficient to account for the functional properties of these crystallins[25,26]. Nevertheless, this study demonstrates for the first time a biochemical function of a Bcl-2-related protein. The regulation of membrane permeability by Bcl-2-related proteins may be important for their ability to modulate cell survival in response to diverse stimuli. □

Methods

Protein purification. Recombinant human Bcl-x_L protein containing a six amino-acid C-terminal histidine tag was expressed in *Escherichia coli* strain HMS174(ÐE3) and purified by affinity chromatography on a nickel-IDA column (Invitrogen) as previously described[5]. Further purification was achieved by ion-exchange chromatography on a Q column. The Bcl-x_L used in this study lacks the C-terminal transmembrane region. Additional studies that gave similar results were performed on a Bcl-x_L mutant that also lacks an unstructured region comprising amino acids 45–84, which was previously shown to be dispensable for anti-apoptotic activity[5].

Synthetic lipid vesicle studies. Large unilamellar vesicles composed of 40% 1,2 dioleoylphosphatidylglycerol and 60% 1,2 dioleoylphosphatidylcholine (Avanti Polar Lipids) were prepared as previously described[27]. The resulting liposomes were then diluted 200-fold to a concentration of 0.05 mg ml^{-1} in 10 mM dimethylglutarate, 100 mM choline nitrate[27] and 2 mM $CaNO_3$ titrated to the appropriate pH with NaOH. Valinomycin was added at 15 nM to generate an inside-negative Nernst diffusion potential[27]. Valinomycin is a K^+-selective ionophore which can establish a transmembrane potential in the absence of a significant change in the K^+ concentrations inside or outside of the vesicles[28]. Bcl-x_L was added at a concentration ranging from 500 ng ml^{-1} to 10 μg ml^{-1}. Cl^- efflux was measured with a Cl^--specific electrode (Orion 94-17B) coupled to a double-junction calomel reference electrode (Orion 90-02). K^+ efflux was measured with a K^+-specific electrode (Orion 93-19).

Planar lipid bilayer studies. Planar lipid bilayers were formed across a 200-μM diameter aperture in the wall of a Delrin cup. Lipid bilayer-forming solution contained 40% phosphatidylserine and 60% phosphatidylcholine (Avanti Polar Lipids) at a concentration of 50 mg ml^{-1} in *n*-decane. Protein was added to one side of the bilayer, defined as *cis*. The concentration of protein added ranged from 3 μg ml^{-1} to 78 μg ml^{-1}. The other side of the bilayer was defined as *trans* and was the virtual ground. Solutions contained 150:15 mM KCl (*cis*:*trans*) and were buffered at either pH 4.0 with 50 mM $NaC_2H_3O_2$ or pH 7.2 with 10 mM HEPES. Both the *cis* and the *trans* compartments were connected to separate chambers containing a $AgCl_2$ electrode by a KCl bridge. A custom current/voltage conversion amplifier was used to optimize single-channel recording[29]. The data were digitized at 2–4 kHz and filtered at 0.75–1.0 kHz using a 12 bit A/D-D/A converter (Axon Instruments) and an 8-pole Bessel filter, except for data demonstrating the time to the onset of current activity, which was digitized at 300 Hz and filtered at 5 Hz. Data were acquired and analysed using pClamp software (Axon Instruments). Curve fits were done using the Marquardt least-squares algorithm.

Received 31 October; accepted 20 December 1996.

1. White, E. *Genes Dev.* **10,** 1–15 (1996).
2. Yang, E. & Korsmeyer, S. J. *Blood* **88,** 386–401 (1996).
3. Lithgow, T., van Driel, R., Bertram, J. F. & Strasser, A. *Cell Growth Differ.* **5,** 411–417 (1994).
4. Krajewski, S. *et al. Cancer Res.* **53,** 4701–4714 (1993).
5. Muchmore, S. W. *et al. Nature* **381,** 335–341 (1996).
6. London, E. *Biochim. Biophys. Acta* **1113,** 25–51 (1992).
7. Cramer, W. A. *et al. Annu. Rev. Biophys. Biomol. Struct.* **24,** 611–641 (1995).
8. Chen-Levy, Z. & Cleary, M. L. *J. Biol. Chem.* **265,** 4929–4933 (1990).
9. Nguyen, M., Millar, D. G., Yong, V. W., Korsmeyer, S. J. & Shore, G. C. *J. Biol. Chem.* **268,** 25265–2526 (1993).
10. Parker, M. W. & Pattus, F. *Trends Biochem. Sci.* **18,** 391–395 (1993).
11. Choe, S. *et al. Nature* **357,** 216–222 (1992).
12. Davidson, V. L., Heymann, J. B., Zhang, Y. L. & Cohen, F. S. *J. Membr. Biol.* **79,** 105–118 (1984).
13. Zakharov, S. D., Heymann, J. B., Zhang, Y. L. & Cramer, W. A. *Biophys. J.* **70,** 2774–2783 (1996).
14. Lam, M. *et al. Proc. Natl Acad. Sci. USA* **91,** 6569–6573 (1994).
15. Zhu, W. *et al. EMBO J.* **15,** 4130–4141 (1996).
16. Perez-Terzic, C., Pyle, J., Jaconi, M., Stehno-Bittel, L. & Clapham, D. E. *Science* **273,** 1875–1877 (1996).
17. Mannella, C. A. *Trends Biochem. Sci.* **17,** 315–320 (1992).
18. Zoratti, M. & Szabo, I. *Biochim. Biophys. Acta* **1241,** 139–176 (1995).
19. Zamzami, N. *et al. J. Exp. Med.* **183,** 1533–1544 (1996).
20. Liu, X., Kim, C. N., Yang, J., Jemmerson, R. & Wang, X. *Cell* **86,** 147–157 (1996).
21. Martin, S. J. & Green, D. R. *Cell* **82,** 349–352 (1995).
22. Slatin, S. L., Abrams, C. K. & English, L. *Biochem. Biophys. Res. Commun.* **169,** 765–772 (1990).
23. Hoch, D. H. *et al. Proc. Natl Acad. Sci. USA* **82,** 1692–1696 (1985).
24. Raymond, L., Slatin, S. L. & Finkelstein, A. *J. Membr. Biol.* **84,** 173–181 (1985).
25. Wistow, G. *Trends Biochem. Sci.* **18,** 301–306 (1993).
26. Tomarev, S. I. & Piatigorsky, J. *Eur. J. Biochem.* **235,** 449–465 (1996).
27. Peterson, A. A. & Cramer, W. A. *J. Membr. Biol.* **99,** 197–204 (1987).
28. Cramer, W. A. & Knaff, D. B. *Energy Transduction in Biological Membranes, a Textbook of Bioenergetics* (Springer, New York, 1990).
29. Györke, S. & Fill, M. *Science* **260,** 807–809 (1993).

Acknowledgements: A.J.M. and P.V. contributed equally to this work. We thank R. Miller, C. Rudin, C. Duckett, B. Chang, M. Vander Heiden and T. Lindsten for discussions and review of the manuscript. We also thank M. Cortéz for technical assistance, and T. Conway and D. Wang for editorial assistance. This work was supported by grants from the NIH and the Howard Hughes Medical Institute.

Correspondence should be addressed to either M.F. (e-mail: mfill@luc.edu) or C.B.T. (e-mail: cthompso@midway.uchicago.edu).

The C-terminal domain of RNA polymerase II couples mRNA processing to transcription

Susan McCracken, Nova Fong, Krassimir Yankulov, Scott Ballantyne*, Guohua Pan†, Jack Greenblatt†, Scott D. Patterson‡, Marvin Wickens* & David L. Bentley

Amgen Institute, 620 University Avenue, Suite 706, Toronto, Ontario M5G 2C1, Canada

* *Department of Biochemistry, University of Wisconsin, 420 Henry Mall, Madison, Wisconsin 53706-1569, USA*

† *Banting and Best Department of Medical Research and Department of Molecular and Medical Genetics, University of Toronto, Ontario M5G 1L6, Canada*

‡ *Amgen Inc., Department of Protein Structure, 1840 DeHavilland Drive, Thousand Oaks, California 91320, USA*

Messenger RNA is produced by RNA polymerase II (pol II) transcription, followed by processing of the primary transcript. Transcription, splicing and cleavage–polyadenylation can occur independently *in vitro*, but we demonstrate here that these processes are intimately linked *in vivo*. We show that the carboxy-terminal domain (CTD) of the pol II large subunit is

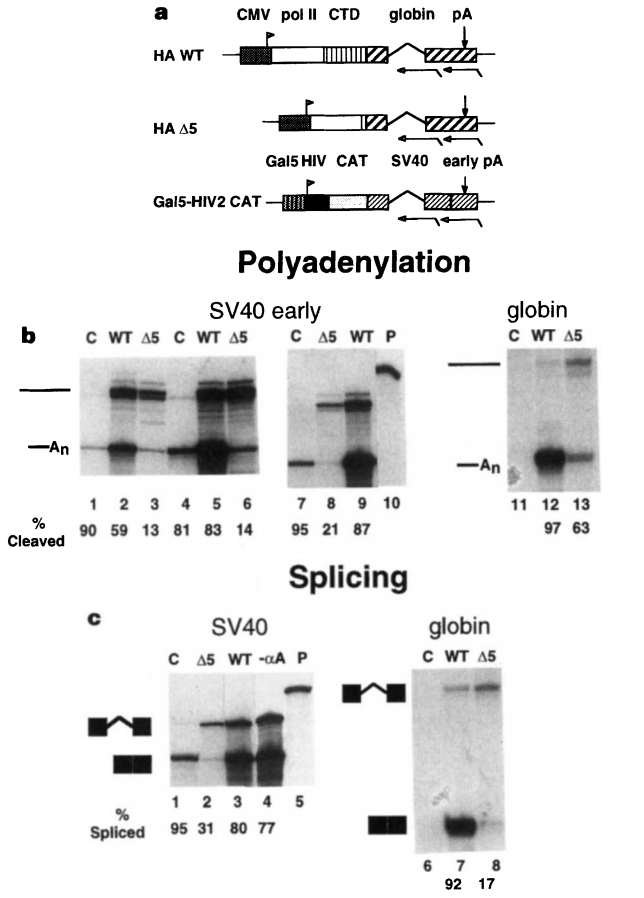

Figure 1 CTD truncation inhibits 3′ processing and splicing. **a**, Wild-type (WT) and CTD-truncated (Δ5) pol II expression plasmids and Gal5–HIV2 CAT reporter. **b**, RNAse protection of cleavage at the SV40 early (lanes 1–9) and rabbit β-globin (lanes 11–13) poly(A) sites. Transcription was activated by Gal4–Sp1 (lanes 1–3) or Gal4–VP16 (lanes 4–9). In lanes 7–9, Gal5–HIV2 CAT was transfected after addition of α-amanitin (see Methods). C, CMV *neo* control; P, probe. **c**, RNAse protection of splicing at the SV40-t intron (lanes 1–4) and rabbit β-globin intron 2 (lanes 6–8). Lanes 1–3 are the same RNAs as in **b**, lanes 7–9. Lanes 1, 2 were exposed for twice as long as lane 3. Lane 4, control without pol II plasmid or α-amanitin.

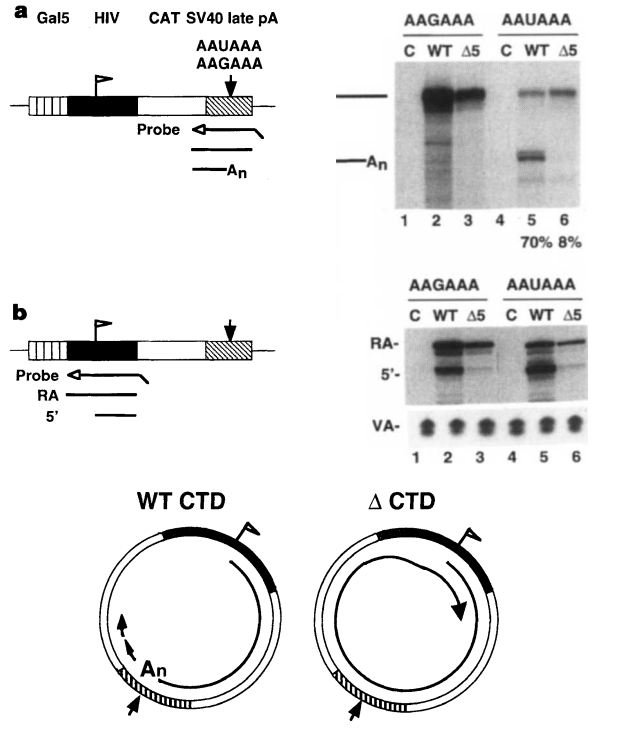

Figure 2 **a**, RNAse protection of SV40 late poly(A) site processing in pre-mRNAs without introns. Transcription of Gal5–HIV2 CAT-AAUAAA and Gal5–HIV2 CAT-AAGAAA was activated by Gal4–VP16. **b**, RNAse protection of the same samples as in **a**, with a 5′ probe, shows accumulation of read-around (RA) transcripts relative to 5′ ends (5′) when AAUAAA is mutated and when the CTD is truncated. Diagram shows the effect of CTD truncation on RA transcription.

required for efficient RNA processing. Splicing, processing of the 3′ end and termination of transcription downstream of the poly(A) site, are all inhibited by truncation of the CTD. We found that the cleavage–polyadenylation factors CPSF and CstF specifically bound to CTD affinity columns and copurified with pol II in a high-molecular-mass complex. Our demonstration of an association between the CTD and 3′-processing factors, considered together with reports of a similar interaction with splicing factors[1,2], suggests that an mRNA 'factory' exists which carries out coupled transcription, splicing and cleavage–polyadenylation of mRNA precursors.

To study the role of the CTD in mRNA production, we transiently transfected cells with vectors expressing α-amanitin-resistant forms of the murine pol II large subunit which had either 5 or 52 heptad repeats in the CTD (consensus, YSPTSPS). These two forms are referred to as Δ5 (or ΔCTD) and wild type (WT), respectively (Fig. 1a)[3]. After a short period of expression, α-amanitin was added to inhibit the host cell's pol II. Using this strategy, it was shown that *in vivo*, as *in vitro*[4], CTD truncation does not affect the accuracy of initiation but reduces the response to enhancers[3]. We initially analysed transcripts of a chloramphenicol acetyltransferase (CAT) reporter gene made by wild-type and ΔCTD pol II and found, surprisingly, that RNA cleavage at the SV40-early poly(A) site was severely inhibited by truncation of the CTD (Fig. 1b; compare Δ5 lanes 3, 6 and 8 with WT lanes 2, 5 and 9). Inhibition of 3′ processing was observed with both strong and weak transcriptional activators (Gal4–Spl in lane 3 and Gal4–VP16 in lane 6 of Fig. 1b), showing that it is not an indirect effect of reduced initiation by the ΔCTD polymerase. Furthermore, 3′ processing was inhibited even when the CAT reporter was transfected after addition of α-amanitin (Fig. 1b, lanes 7–9). Cleavage at the rabbit β-globin (Fig. 1b, lanes 12, 13) and human α-globin (data not shown) poly(A) sites was also significantly reduced by CTD truncation. We then compared splicing of two introns transcribed by pol II with a wild-type or truncated CTD. Splicing of the SV40-t intron and the rabbit β-globin intron 2 was significantly inhibited by truncating the CTD (Fig. 1c). Splicing was equally efficient in untreated cells and in α-amanitin-treated cells transfected with the wild-type pol II expression vector (Fig. 1c, lanes 3 and 4).

Control experiments were done to eliminate the possibility that inhibition of RNA processing in cells expressing ΔCTD polymerase was due to depletion of unstable processing factors. Inhibition of protein synthesis by addition of cycloheximide plus α-amanitin to cells expressing WT pol II did not affect RNA processing (data not

shown). Furthermore, α-amanitin-treated cells transfected with CMV *neo*, instead of a pol II expression plasmid, produced a small amount of CAT RNA that was correctly spliced and cleaved at the 3′ end (Fig. 1b, lanes 1, 4 and 7; Fig. 1c, lane 1), showing that even a greatly reduced level of overall pol II transcription did not inhibit processing. We conclude that inhibition of RNA processing is specific to transcripts made by pol II with a truncated CTD and not those made by full-length pol II.

Inhibition of 3′ processing by the ΔCTD polymerase could be an indirect effect of inhibiting splicing of the 3′ intron[5,6]. To test this possibility, we analysed two CAT reporter genes with wild-type or mutant SV40-late poly(A) sites but no introns. 3′ processing of the SV40-late poly(A) site was greatly reduced by CTD truncation in the absence of an intron (Fig. 2a, lanes 5 and 6). There was no processing at the AAGAAA mutant site, confirming the sequence specificity of this cleavage reaction (Fig. 2a, lanes 2 and 3). We conclude that inhibition of 3′ processing by CTD truncation cannot be accounted for as a secondary effect of reduced splicing.

The AAUAAA and G/U rich elements that are required for 3′ processing are also necessary for transcriptional termination, which usually occurs far downstream of the poly(A) site[7–9]. Mutation of these motifs can cause RNA polymerase II to read around the entire plasmid several times because of failure to terminate[7]. Read-around (RA) transcripts are distinguished in an RNase protection assay because they protect a region of the probe that extends upstream and downstream of the start site (Fig. 2b). Even in the presence of a wild-type AAUAAA motif, read-around transcripts accumulated when the gene was transcribed by the ΔCTD polymerase (Fig. 2b, lane 6, and lower panel). This observation shows that although a wild-type AAUAAA is necessary for pol II termination, it is not sufficient in the absence of the CTD.

To pursue the biochemical basis of the functional link between the CTD and 3′ RNA processing, we investigated whether cleavage–polyadenylation factors bind to this domain. HeLa cell nuclear extract was chromatographed sequentially on affinity columns of glutathione *S*-transferase (GST) and the fusion proteins GST-mutant CTD, GST–wild-type CTD and hyperphosphorylated GST–wild-type CTD (Fig. 3a, lanes 1–4). High-salt eluates of the columns were analysed by western blotting with antibodies against two subunits of CstF and three subunits of CPSF, as well as against poly(A) polymerase (Fig. 3b). CstF and CPSF, but not poly(A) polymerase, bound to hypo- and hyperphosphorylated wild-type CTD but not to GST or mutant CTD. Although similar profiles of total protein eluted from all three CTD columns (Fig. 3a, lanes 8–10), CstF and CPSF were found specifically in the eluates from the two wild-type columns. The fraction of CstF and CPSF that bound the CTD differed between subunits, possibly reflecting unequal amounts of these polypeptides in the HeLa cell extract. CstF and CPSF coimmunoprecipitate (S.M. and D.B., unpublished results) and may bind to the CTD as a complex. Significant binding of TBP[10], perhaps as a component of the TFIID complex, but not of TFIIB, TFIIE or TFIIF, to the CTD was also detected (Fig. 3b).

CstF binding to the CTD was investigated by translation of its three subunits *in vitro*, followed by binding to GST resins. The p50 subunit bound very efficiently to wild-type CTD but not to GST or mutant CTD (Fig. 3c). The p77 subunit also bound specifically to the CTD but much less efficiently than p50, and p64 did not bind at all. The p50 subunit has seven β-transducin (WD40) repeats at its C terminus (residues 93–431)[11]. Incomplete translation products (Fig. 3c, top) and a C-terminally deleted form with 2.5 β-transducin repeats (residues 1–211) bound to the CTD weakly compared with full-length p50 (Fig. 3c). CTD binding was severely reduced by N-terminal deletion of residues 1–91 of p50 (Fig. 3c), indicating that the β-transducin repeats are not sufficient for CTD binding.

If 3′-processing factors stably associate with the CTD *in vivo*, they may copurify with pol II. In mammalian cells, pol II exists as high-molecular-mass holoenzyme complexes containing general transcription factors (GTFs)[12,13]. Holoenzyme was prepared by affinity chromatography on GST–TFIIS, followed by gel filtration; this complex contains TFIID and all the general transcription factors required for initiation (G.P., T. Aso and J.G., manuscript submitted). Western blotting of the eluate from the GST–TFIIS column (Fig. 4, left) showed retention of CPSF (p160) and CstF (p64 and p77) but not of poly(A) polymerase or the coactivator CBP. Gel filtration of the GST–TFIIS eluate (Fig. 4, right) showed that pol II, TFIIF (rap 74), TFIIH (ERCC3), cyclin C (data not shown) and CstF cofractionated precisely, peaking in fraction 24 with an apparent relative molecular mass (M_r) greater than 2,000K. CPSF copurified extensively with pol II but its peak was in fraction 23, probably because there is some heterogeneity of the complexes.

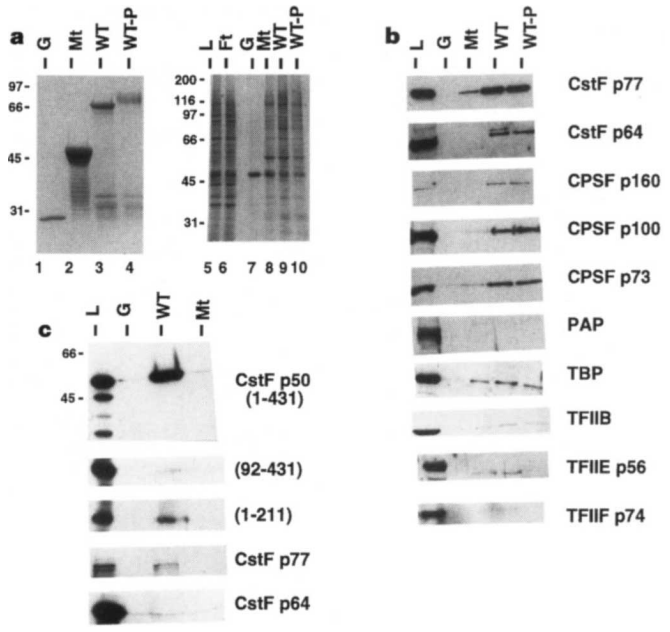

Figure 3 CPSF and CstF bind specifically to the CTD. **a**, Lanes 1–4, Coomassie stain of GST(G), GST-CTD mutant (Mt), GST-CTD wild type (WT) and GST-CTD hyperphosphorylated (WT-P) affinity resins. Lanes 5–10, silver stain of load (L, 0.5 μl), flow-through (Ft, 0.5 μl) and 0.6 M NaCl eluates (15 μl). **b**, Western blots of load (0.083%, 5 μl) and column eluates (1%, 5 μl). Note that anti-TFIIE detected a lower-M_r artefact band in addition to p56. **c**, Binding of ^{35}S-Met-labelled *in vitro* translated CstF subunits to the CTD. 10% of the input (L) and 50% of the bound fractions are shown.

Our results demonstrate that a full-length RNA pol II CTD is required for efficient splicing and 3′ processing *in vivo*. The binding of 3′-processing factors to the CTD provides a plausible molecular explanation for the functional coupling of transcription with cleavage–polyadenylation. CPSF/CstF binding to the CTD probably promotes recruitment to the RNA substrate and thereby enhances the cleavage reaction. This effect can explain why pol I (ref. 14, and D. Zarkower and M.W., unpublished results), pol III (ref. 15) and T7 RNA polymerase (ref. 16, and N.F. and D.B., unpublished results), which lack a CTD, do not produce mRNAs that are efficiently cleaved and polyadenylated.

After completing synthesis of the pre-mRNA, pol II terminates transcription in an AAUAAA-dependent manner. The mechanism that couples termination to polyadenylation is unknown[7–9]. Our observations that the AAUAAA signal and the CTD are both required for termination (Fig. 2b) and that 3′-processing factors bind to phosphorylated and non-phosphorylated CTD (Fig. 3b) suggest a solution to this problem (Fig. 5). We propose that CPSF and CstF, as well as splicing factors[1,2], travel with the hyperphosphorylated elongating polymerase. The CPSF/CstF interaction

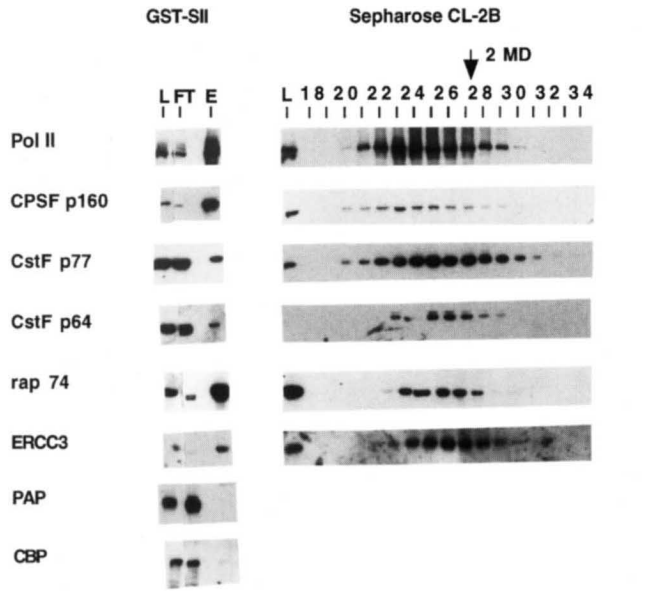

Figure 4 CstF and CPSF copurify with pol II holoenzyme. This complex was purified by affinity chromatography of HeLa extract on GST-TFIIS (SII) and gel filtration on Sepharose CL-2B. Western blots of load (L), flow-through (FT) and 0.325 M NaCl eluate (E) from the GST-TFIIS column (left) and the load (L) and gel-filtration column fractions (right). The 2-megadalton Dextran-blue 2000 marker (2 MD; Pharmacia) is indicated. Equal signals for the GST-TFIIS load and eluate fractions signify 1.5% binding.

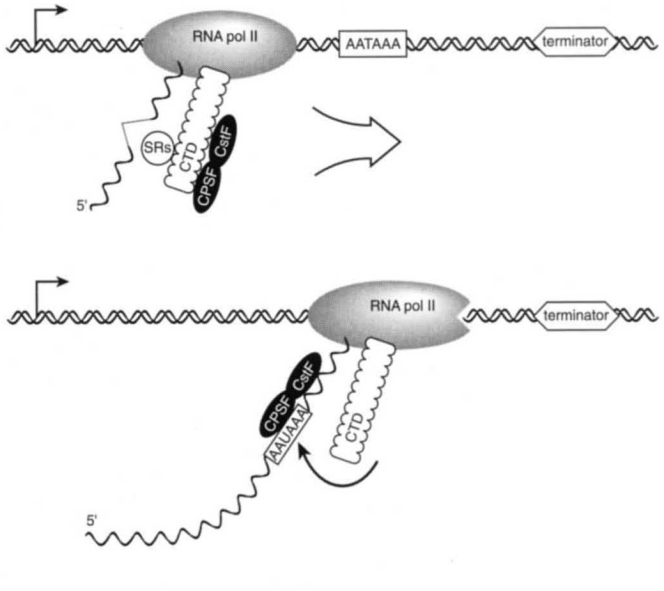

Figure 5 Top, model for an mRNA factory capable of RNA synthesis and processing. Bottom, alteration or reversal of CPSF/CstF binding to the CTD at the poly(A) site switches pol II into a termination-competent state.

with the CTD is altered or disrupted when the polymerase transcribes the polyadenylation signal and processing factors bind to the RNA transcript. The altered interaction of the CTD with 3′-processing factors could signal a switch in the polymerase to a termination-competent state. This model is analogous to the modulation of *Escherichia coli* RNA polymerase elongation through binding of phage lambda N protein to the nascent RNA.

The effect of the CTD on splicing (Fig. 1c) may be due to recruitment of splicing factors to the pre-mRNA via protein–protein interactions with the CTD[17]. Our results are consistent with observations of co-transcriptional splicing *in vivo*[18,19] and corroborate recent reports demonstrating an association of SR-family splicing factors with the CTD (refs 1 and 2, and S.M. and D.B., data not shown) and inhibition of *in vitro* splicing by a CTD peptide[1].

Functional[5,6] and biochemical[20,21] association between the splicing and 3′-processing machineries has been established. Furthermore, sites of transcription in the nucleus colocalize with sites of splicing[22,23] and with a fraction of the polyadenylation factor CstF64 (ref. 24). We propose that splicing and polyadenylation are not only coupled to one another, but also to transcription. In particular, we suggest that mature transcripts are produced in an mRNA 'factory' in which the transcriptional, splicing and cleavage–polyadenylation machineries interact through contacts with the pol II CTD (Fig. 5). The copurification of polyadenylation factors with an initiation-competent form of pol II holoenzyme suggests that the 'factory' may be in place at the promoter. This complex is effectively an assembly line that enhances mRNA production by channelling precursors directly from the synthetic machinery to the processing machinery. □

Methods

Transfection and RNA analysis. 293 cells were transfected with 5 μg Gal5–HIV2 CAT reporter, 0.5 μg pSPVA, 5 μg pol II expression vector[3] or CMV *neo* and 1 μg Gal4 fusion vector by $Ca_3(PO_4)_2$ precipitation. α-amanitin (2.5 μg ml^{-1}) was added after 12–15 h and cells were collected after 65 h. Mock-transfected and ΔCTD-expressing cells survive at least three days in α-amanitin. In Fig. 1b, lanes 7–9, and Fig. 1c, lanes 1–3, the Gal5–HIV2 CAT reporter was introduced after 24 h in a second transfection 1 h after addition of α-amanitin. RNA was collected after 72 h for RNAse protection[25]. Antisense riboprobes: SV40 early poly(A) site, *Ssp*I-linearized pGcat2.2 (ref. 26); SV40 late poly(A) site, PCR fragments of Gal5–HIV2 CAT-AAGAAA/AAUAAA (−205 to +70 relative to AAUAAA); SV40 t-antigen intron 3′ splice site, 345-bp *Apo*I–*Ssp*I fragment; rabbit β-globin poly(A), 220-bp *Eco*RI–*Nde*I fragment; rabbit β-globin intron-2 3′ splice site, 180-bp *Apa*I–*Bgl*II fragment. VA1 RNA was analysed as described[25]. Gel bands were quantified by Phosphorimager (Molecular Dynamics) and corrected for U content.

Affinity chromatography. GST fusion proteins were immobilized at 4 mg ml^{-1}, except for the mutant CTD, which was at 8 mg ml^{-1}. The mutant CTD has 15 repeats of YSPTAPS[27]; the wild-type has all 52 repeats of murine pol II (ref. 28). GST–CTD resin was phosphorylated with total HeLa nuclear extract. Antibodies raised against this material specifically recognized pol IIO. For Fig. 3b, HeLa nuclear extract[29] (33 mg in 6 ml buffer D with 0.1M KCl instead of NaCl) was passed sequentially over four 0.2-ml columns at 4 °C, washed with 2 ml buffer D-0.1M KCl and eluted with 0.5 ml of buffer D-0.6M NaCl. 0.3–0.4% of total protein bound to each CTD resin. Ethidium bromide and RNase did not affect CPSF or CstF binding.

^{35}S-Met-labelled CstF p50, p64 and p77 were made by TNT (Promega) from full-length rat cDNAs. The C-terminal deletion (residues 1–211) of p50 was made by linearizing with *Dra*I and the N-terminal deletion (92–431) was made by subcloning an *Aat*II–*Stu*I fragment into pET21d. Translations were diluted 1:10 in 20% glycerol, 100 mM NaCl, 0.05% non-fat dry milk, 0.1% N-P40, 400 μg ml^{-1} ethidium bromide, 20 mM HEPES, pH 7.9, 0.1 mM EDTA, 2 mM DTT, and bound to GST resins (25 μl) for 1 h at 25 °C, washed 3 times with 0.5 ml binding buffer and eluted in 0.6M NaCl.

Antibodies. Anti-p64, anti-PAP and anti-p160 were provided by J. Manley, anti-p100 and anti-p73 (ref. 30) by A. Jenny and W. Keller, anti-ERCC3 by J.-M. Egly, and anti-TFIIB by P. O'Hare; anti-CBP (A-22) was from Santa Cruz Biotechnology and anti-TBP was from Upstate Biotechnology. Anti-TFIIE(p56), anti-TFIIF(rap74) and anti-CstF 77 and anti-PAP peptide antisera were raised in rabbits and affinity-purified.

Pol II holoenzyme. Holoenzyme was prepared as described (G.P., T. Aso and

J.G., manuscript submitted). HeLa whole-cell extract (200 mg) in CHB buffer (10 mM HEPES, pH 7.9, 0.2 mM EDTA, 0.2 mM EGTA, 5 mM β-glycerophosphate, 1 mM DTT, 50 μM $ZnCl_2$, 0.05% N-P40, 12% glycerol) plus 50 mM NaCl was chromatographed on a 1-ml GST–TFIIS column (10 mg per ml ligand), washed with 15 ml CHB-50 mM NaCl, then eluted with CHB-325 mM NaCl. 2 ml of eluate was loaded onto a Sepharose CL-2B column (60 × 1.6 cm; flow rate 0.4 ml min^{-1}) equilibrated with CHB-100 mM NaCl plus 8% glycerol, and 4-ml fractions were collected.

Received 31 July; accepted 22 November 1996.

1. Yuryev, A. *et al. Proc. Natl Acad. Sci. USA* **93,** 6975–6980 (1996).
2. Mortillaro, M. J. *et al. Proc. Natl Acad. Sci. USA* **93,** 8253–8257 (1996).
3. Gerber, H. P. *et al. Nature* **374,** 660–662 (1995).
4. Zehring, W. A., Lee, J. M., Weeks, J. R., Jokerst, R. S. & Greenleaf, A. L. *Proc. Natl Acad. Sci. USA* **85,** 3698–3702 (1988).
5. Nesic, D., Cheng, J. & Maquat, L. E. *Mol. Cell. Biol.* **13,** 3359–3369 (1993).
6. Niwa, M., Rose, S. D. & Berget, S. M. *Genes Dev.* **4,** 1552–1559 (1990).
7. Connelly, S. & Manley, J. L. *Genes Dev.* **2,** 440–452 (1988).
8. Logan, J., Falck, P. E., Darnell, J. E. J. & Shenk, T. *Proc. Natl Acad. Sci. USA* **84,** 8306–8310 (1987).
9. Whitelaw, E. & Proudfoot, N. *EMBO J.* **5,** 2915–2922 (1986).
10. Usheva, A. *et al. Cell* **69,** 871–881 (1992).
11. Takagaki, Y. & Manley, J. L. *J. Biol. Chem.* **267,** 23471–23474 (1992).
12. Ossipow, V., Tassan, J. P., Nigg, E. A. & Schibler, U. *Cell* **83,** 137–146 (1995).
13. Maldonado, E. *et al. Nature* **381,** 86–89 (1996).
14. Smale, S. T. & Tijan, R. *Mol. Cell. Biol.* **5,** 5352–5362 (1985).
15. Sisodia, S. S., Sollner, W. B. & Cleveland, D. W. *Mol. Cell. Biol.* **7,** 3602–3612 (1987).
16. Mifflin, R. C. & Kellems, R. E. *J. Biol. Chem.* **266,** 19593–19598 (1991).
17. Greenleaf, A. L. *Trends Biochem. Sci.* **18,** 117–119 (1993).
18. Beyer, A. L. & Osheim, Y. N. *Genes Dev.* **2,** 754–765 (1988).
19. Wuarin, J. & Schibler, U. *Mol. Cell Biol.* **14,** 7219–7225 (1994).
20. Lutz, C. S. *et al. Genes Dev.* **10,** 325–337 (1996).
21. Boelens, W. C. *et al. Cell.* **72,** 881-892 (1993).
22. Zhang, G., Taneja, K. L., Singer, R. H. & Green, M. R. *Nature* **372,** 809–812 (1994).
23. Mattaj, I. W. *Nature* **372,** 727–728 (1994).
24. Schul, W. *et al. EMBO J.* **15,** 2883–2892 (1996).
25. Blau, J. *et al. Mol. Cell. Biol.* **16,** 2044–2055 (1996).
26. Lieber, A., Kiessing, U. & Strauss, M. *Nucleic Acids Res.* **17,** 8485–8493 (1989).
27. West, M. & Corden, J. *Genetics* **140,** 1223–1233 (1995).
28. Peterson, S. R., Dvir, A., Anderson, C. W. & Dynan, W. S. *Genes Dev.* **6,** 426–438 (1992).
29. Dignam, J. D., Lebovitz, R. M. & Roeder, R. G. *Nucleic Acids Res.* **11,** 1475–1489 (1983).
30. Jenny, A., Minvielle-Bastia, L., Preker, P. & Keller, W. *Science* **274,** 1514–1517 (1996).

Acknowledgements: S.McC., N.F. and K.Y. contributed equally to this work. We thank J. Blau, P. Atadja and B. McNeil for their contribution; J. Corden, M. West and A. Yuryev for plasmids and for sharing unpublished data; R. Treisman and L. Harrington for discussion. J. Manley, W. Keller, A. Jenny, P. O'Hare, E. Lees, J.-M. Egly, M. Rihanek, T. Zamborelli, M. Pandes, J. Biron, S. Suggs and the Amgen EST Program for antibodies, HeLa cells and CstF plasmids; and A. Hessel, H. Agah, M. Pandes, P. Courchesne, B. Bolychuk and S. Pang for computer, technical, photographic and secretarial assistance.

Correspondence and requests for materials to D.B. (e-mail: david.bentley@amgen.com).

Structure of the conserved GTPase domain of the signal recognition particle

Douglas M. Freymann, Robert J. Keenan, Robert M. Stroud & Peter Walter

Department of Biochemistry and Biophysics, School of Medicine, University of California, San Francisco, California 94143-0448, USA

The signal-recognition particle (SRP) and its receptor (SR) function in the co-translational targeting of nascent protein–ribosome complexes to the membrane translocation apparatus[1]. The SRP protein subunit (termed Ffh in bacteria) that recognizes the signal sequence of nascent polypeptides is a GTPase, as is the SR-α subunit (termed FtsY)[2,3]. Ffh and FtsY interact directly, each stimulating the GTP hydrolysis activity of the other[4]. The sequence of Ffh suggests three domains: an amino-terminal N domain of unknown function, a central GTPase G domain, and a methionine-rich M domain that binds both SRP RNA and signal peptides[5,6]. Sequence conservation suggests that structurally similar N and G domains are present in FtsY[7,8]. Here we report the structure of the nucleotide-free form of the NG fragment of Ffh. Consistent with a role for apo Ffh in protein targeting, the side chains of the empty active-site pocket form a tight network of interactions which may stabilize the nucleotide-free protein. The structural relationship between the two domains suggests that the N domain senses or controls the nucleotide occupancy of the GTPase domain. A structural subdomain unique to these evolutionarily conserved GTPases constitutes them as a distinct subfamily in the GTPase superfamily[9].

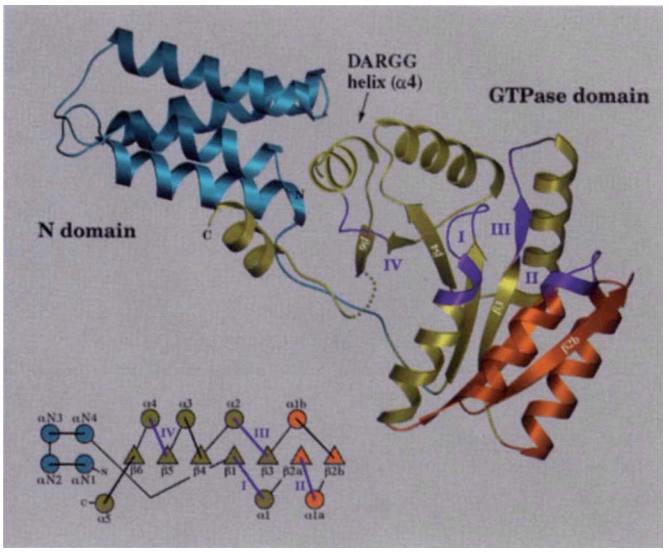

Figure 1 Structure and topology of the NG domain. The four-helix bundle of the N domain (blue) is closely associated with the GTPase domain (green and orange). The loops containing the conserved GTPase sequence motifs I (105–112), II (135–141), III (187–192), and IV (245–248) are highlighted (purple); these define the position of the GTP-binding site. The interface between the two domains occurs primarily along a single, distorted helix (the 'DARGG' helix). The main structural difference distinguishing the GTPase of Ffh from other GTPases is the subdomain, coloured orange, inserted between helix α1 and strand β3 of the core GTPase fold. The α-helices and β-strands are numbered in accordance with their structural counterparts in $p21^{ras}$. An eight-residue loop cannot be seen in the electron-density map and is probably disordered because of the absence of bound nucleotide; it is indicated by the dotted line.

The structure of the apo form of Ffh NG (Fig. 1) was determined to a resolution of 2.05 Å by X-ray diffraction using multiple isomorphous replacement (Table 1). The G domain has a β/α fold that is structurally similar to other GTPases in the superfamily including $p21^{ras}$ (Ras)[10], EF-G[11,12] and transducin Gα[13]. The N domain is a bundle of four antiparallel α-helices, which open at one end, allowing sidechains of the G domain to complete the packing of its hydrophobic core. The protein is thus a single structural unit in which the two sequence domains, N and G, are distinct, yet closely associated. A ten-residue peptide that links the two domains is packed tightly against the protein surface, rendering the NG fragment stable to proteolysis[5,14].

The core GTPase fold is a five-stranded β-sheet surrounded by α-helices; loops between the β-strands of the sheet and the α-helices contain four highly conserved sequence motifs (I–IV) which mediate interaction with the bound ribonucleotide[15] (Fig. 1, purple). Two striking structural differences distinguish the G domain of Ffh from other subfamilies of GTPases. The first is the subdomain (Fig. 1, orange), which includes motif II (G–2)[15]; this region is highly conserved within, but not between, subfamilies of GTPases, and in Ras and other GTPases it is known to interact with GTPase-activating proteins[9]. As Ffh and FtsY mutually stimulate GTP hydrolysis[4], the subdomain is likely to function in the interaction between the Ffh and its receptor. It is an insertion of 50 amino acids that extends the core β-sheet by two strands and two helices to form a seven-stranded all-parallel β-sheet. The first